High-throughput mass spectrometric N-glycomics

Reiding, K.R.

Chapter 4

Automation of high-throughput mass spectrometry-based plasma *N*-glycome analysis

Technical note

Karli R. Reiding[1†], Marco R. Bladergroen[1†], Agnes L. Hipgrave Ederveen[1], Gerda C. M. Vreeker[1], Florent Clerc[1], Stephanie Holst[1], Albert Bondt[1,2], Manfred Wuhrer[1,3], Yuri E. M. van der Burgt[1]

†These authors contributed equally

[1]Center for Proteomics and Metabolomics, Leiden University Medical Center (LUMC), PO Box 9600, 2300 RC Leiden, The Netherlands;

[2]Department of Rheumatology, Erasmus University Medical Center, 3000 CA Rotterdam, The Netherlands;

[3]Division of BioAnalytical Chemistry, VU University Amsterdam, 1081 HV Amsterdam, The Netherlands;

Reprinted and adapted with permission from J. Proteome Res., 2015, 14 (9), pp 4080–4086; DOI: 10.1021/acs.jproteome.5b00538; Publication Date (Web): July 16, 2015

4.1 Abstract

Glycosylation is a post-translational modification of key importance with heterogeneous structural characteristics. Previously, we have developed a robust, high-throughput MALDI-TOF–MS method for the comprehensive profiling of human plasma *N*-glycans. In this approach, sialic acid residues are derivatized with linkage-specificity, namely the ethylation of α2,6-linked sialic acid residues with parallel lactone formation of α2,3-linked sialic acids. In the current study, this procedure was used as a starting point for the automation of all steps on a liquid-handling robot system. This resulted in a time-efficient and fully standardized procedure with throughput times of 2.5 h for a first set of 96 samples and approximately 1 h extra for each additional sample plate. The mass analysis of the thus-obtained glycans was highly reproducible in terms of relative quantification, with improved interday repeatability as compared to that of manual processing.

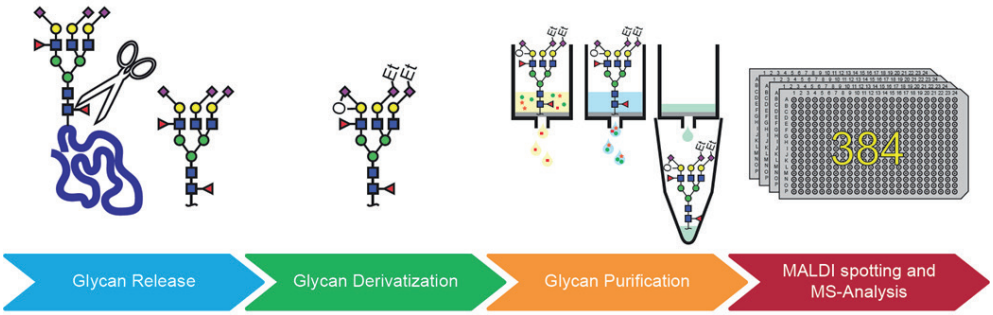

4.2 Introduction

Glycosylation is an important post-translational protein modification with significant effects on, for example, conjugate stability, folding, solubility, and receptor interaction[1-3]. These effects also apply to biopharmaceuticals, in which glycans have been shown to influence glycoconjugate half-life and biological activity[4,5]. In addition, glycosylation has proven to be reflective of (and in some cases causal to) disease etiology. Notable examples include tumor growth and metastasis, inflammation, and congenital disorders of glycosylation[6-8]. To study glycosylation for the development of biopharmaceuticals and clinical biomarkers, large numbers of samples are required. Sample processing times, however, are often a limiting factor in high-throughput screening studies. This has prompted efforts toward integrated methodology and automated workflows on robotic liquid-handling platforms[9-11].

Matrix-assisted laser desorption/ionization time-of-flight mass spectrometry (MALDI-TOF–MS) is an attractive and high-throughput method for compositional glycan analysis[12,13]. However, such an analysis can be severely hampered by the instability and ionization bias of sialylated glycan species. To overcome these limitations, we recently established a rapid, robust, and linkage-specific high-throughput method for sialic acid stabilization and applied MALDI-TOF–MS analysis to map PNGase F-released human plasma *N*-glycan mixtures[14]. The stabilization and neutralization of these sialic acids was achieved by specific and near-complete carboxyl group derivatization with discrimination between α2,3- and α2,6-linked sialic acids, namely through the ethyl esterification of α2,6-linked sialic acids and lactonization of α2,3-linked variants, leading to the mass-based discrimination of sialylation linkage isomers. Derivatized glycans were then recovered by hydrophilic interaction liquid chromatography (HILIC) solid-phase extraction (SPE) followed by MS analysis. The discrimination of the sialic acid linkages is an important aspect of glycosylation analysis because the isomers may differ in biological functionality. It was, for example, shown that α2,6-sialylation (and not α2,3-sialylation) has an effect on the anti-inflammatory activity of immunoglobulin G, whereas the up-regulation of α2,3-sialylation (and the corresponding increase of sialyl-Lewis X) has been associated with the metastasis of various cancer types[15-17]. The ethyl esterification method has thus far been applied to the in-depth analysis of plasma *N*-glycosylation, as well as to explore the differences between glycans on the IgG variable and constant region and their changes during pregnancy[14-18]. Although the derivatization, SPE, and MALDI measurement can be performed within a few hours for 96 samples, the processing of large cohorts is still time-consuming and tends to result in considerable batch-to-batch variation.

In this paper, we present a fully automated protocol for the high-throughput analysis of *N*-glycans released from plasma proteins with linkage-specific derivatization of sialic acid residues. The protocol makes use of a 96-well filter plate with GH Polypro (GHP) membrane, which has previously been reported to function as the HILIC stationary phase in SPE[19]. Using

a robotic liquid-handling system, 384 samples can be prepared without user intervention within a running time of 5.5 h, followed by MALDI-TOF–MS analysis within an additional 1.5 h. In addition to the beneficial aspect with regard to sample throughput, the automation of this protocol for *N*-glycan release combined with the linkage-specific derivatization of sialic acid residues ensures robustness and standardization.

4.3 Experimental section

Chemicals and reagents

Throughout this study, ultrapure water (MQ) was used (≥18.2 MΩ at 25 °C). Nonidet P-40 substitute (NP-40), 1-hydroxybenzotriazole monohydrate (HOBt), and super-DHB were purchased from Sigma-Aldrich (Steinheim, Germany). Peptide-*N*-glycosidase F (PNGase F) was obtained from Roche Diagnostics (Mannheim, Germany), HPLC-grade acetonitrile (ACN) was purchased from Biosolve (Valkenswaard, The Netherlands), analytical grade ethanol was purchased from Merck (Darmstadt, Germany), and 1-ethyl-3-(3-(dimethylamino)propyl)carbodiimide hydrochloride (EDC) was purchased from Fluorochem (Hadfield, United Kingdom).

Samples

Plasma standard (Visucon-F frozen normal control plasma, pooled from 20 human donors, citrated, and buffered with 0.02 M HEPES) was obtained from Affinity Biologicals (Ancaster, ON) and used for all repeatability experiments.

Glycan release

N-Glycans were enzymatically released from plasma proteins using PNGase F as described previously, with minor modifications[20]. In short, a 6 µL plasma sample was denatured by the addition of 12 µL of 2% SDS and incubation for 10 min at 60 °C. For the glycan release, 12 µL of 2.5× PBS containing 2% NP-40 and 0.4 mU PNGase F were added followed by incubation for 16 h at 37 °C. After glycan release, the 96-well plate was either directly transferred to the robot to prepare samples for MALDI-TOF–MS analysis or stored at −20 °C until further use.

Robotic platform

The automated liquid handling platform used in this study is identical to the robotic system that has been described in detail[21,22]. The platform is depicted in **Figure 1** and consists of three units, namely (1) an 8-channel Hamilton MicrolabSTAR; (2) a Hamilton MicrolabSWAP, plate storage, and automated vacuum centrifuge; and (3) a Hamilton MicrolabSTARplus, hereafter referred to as Unit1, Unit2, and Unit3, respectively. The two pipetting platforms (*i.e.*, Unit1 and Unit3) are controlled by two independent computers that are “mastered” through Hamilton scheduler software on a third computer that also controls Unit2.

A modular design was followed to program such an automated protocol. In each procedure, either one or more units or parts of these units (“resources”, *e.g.*, STAR, STARplus, RVC, SWAP, or a combination of these) are allocated to perform an “activity” as controlled through the scheduler software. An overview of all activities that are applied in a procedure is given in **Figure 2A**. All activities are performed via a programmed method. The first method in a procedure initially creates a unique identifier. User input is then required to set up the procedure. This information included, among others, the activities to be performed (*e.g.*, selecting whether MALDI spotting is required after derivatization and cleanup), the method of MALDI spotting, and sample and matrix volumes in case of MALDI spotting.

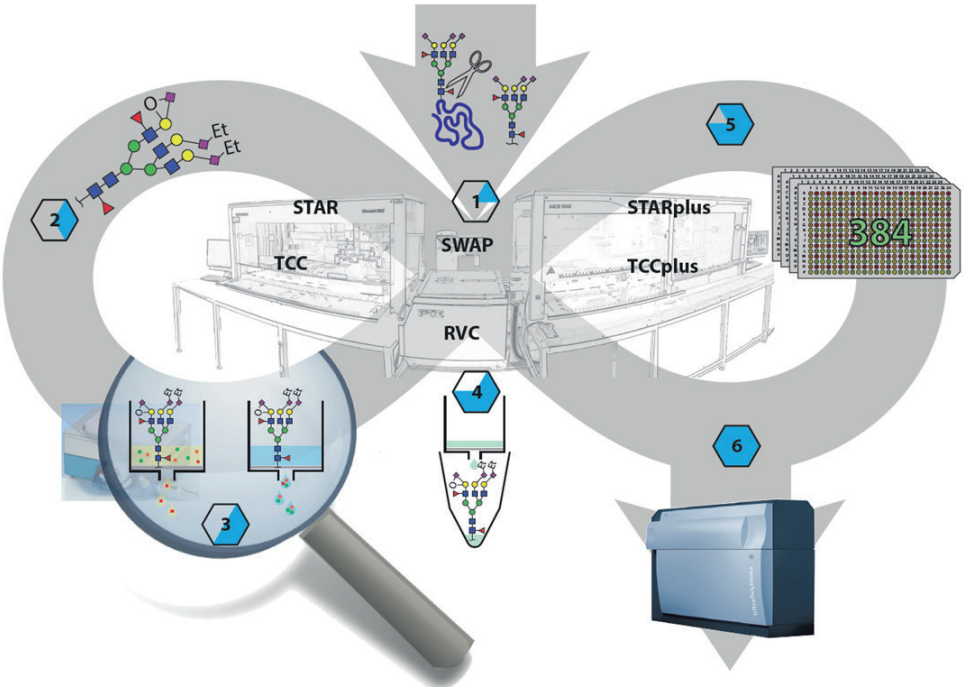

***Figure 1**. Graphical representation of the system setup and the consecutive processing steps locally represented therein: (**1**) PNGase F release, (**2**) ethyl esterification, (**3**) glycan binding and enrichment by GHP HILIC–SPE, (**4**) elution of the glycans from the GHP membrane, (**5**) MALDI target spotting, and (**6**) MALDI-TOF–MS analysis.*

Automated ethyl esterification of released glycans

Before starting a procedure on the robot, freshly prepared chemicals and solutions are supplied to the designated reagent containers. The robotics procedure comprised the following steps: a microtitration plate (96-well PCR plate, polypropylene, Greiner Bio-One, Alphen a/d Rijn, The Netherlands) was filled with 60 µL of ethylation reagent (250 mM EDC and 250 mM HOBt in ethanol) per well. A total of 3 µL of released glycan sample was added, and the plate was covered to prevent solvent evaporation and incubated for 75 min at room

temperature. Before proceeding to purification, 120 µL of ACN was added to the derivatized glycans to prepare the sample for cleanup.

Purification of esterified glycans

A 96-well filter plate with a GHP membrane (GHP plate, Pall AcroPrep Advance 96 Filter plate, Pall Corporation, Ann Arbor, MI) was prewetted, activated, and equilibrated with 100 µL of 70% ethanol, 100 µL of water, and 100 µL of ACN, respectively. The complete volume of the esterification reaction (183 µL) was applied onto the GHP plate, followed by 5 min of incubation, after which the lowest possible vacuum was applied (about 3 kPa below ambient pressure) to ensure a slow flow. The GHP plate was washed three times with 100 µL of 96% ACN. Subsequently, the GHP plate was gently tapped on a disposable hand towel (*e.g.*, Kleenex) to remove residual solvents and transferred onto the top of a PCR plate. For elution, 30 µL of water was added to the filter plate, followed by 5 min of incubation. Recovery was performed by centrifugation at approximately 300 *g* for 5 min.

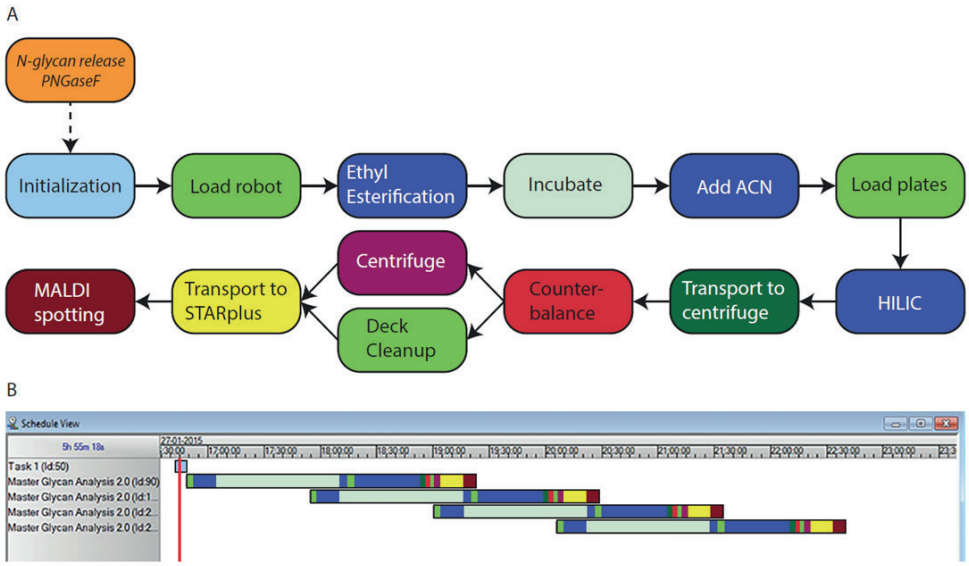

***Figure 2**. Workflow showing the modular setup **A)** and a graphical representation of the scheduled processes for four plates **B)**. Each colored box represents an activity that launches individual programmed methods on the respective resources. The colors in panel A match those in panel B. The resources used are STAR and SWAP (light green); STAR and TCC (dark blue); none (light blue), STAR, RVC, and SWAP (dark green); SWAP and RVC (light red); RVC (purple); SWAP, RVC, STARplus, and TCCplus (yellow); and STARplus and TCCplus (dark red).*

Target plate spotting and MALDI-TOF–MS

Samples were spotted onto a MALDI target plate using the same liquid handling instrument and procedure as described previously[21]. In short, 10 µL of sample was premixed with 10 µL of matrix (5 mg/mL super-DHB in 99% ACN with 1 mM NaOH) in a 384-well plate. A sample

of 2 µL of this mixture was spotted onto a MALDI target plate (800/384 MTP AnchorChip, Bruker Daltonics, Bremen, Germany) and allowed to dry. The MALDI-TOF–MS experiments were performed in reflectron positive mode on an UltrafleXtreme mass spectrometer with a Smartbeam-II laser (Bruker Daltonics) controlled by flexControl 3.4 (Build 135). Within a window of *m/z* 1000 to 5000, spectra were recorded with 10 000 laser shots at a frequency of 1000 Hz, employing a full sample random walking pattern of 100 shots per raster spot.

Method repeatability

To test the repeatability of the automated protocol for the ethyl esterification, purification, MALDI target spotting, and MALDI-TOF–MS analysis of plasma *N*-glycosylation, we prepared a master plate containing 88 released glycan samples (100 µL) originating from a stock solution of mixed releases, as well as 8 PBS blanks. These samples were processed with the robotized method on three different days (2 and 8 days apart) to establish the interday variability (day 1–3), as well as three times within those days to establish the intraday variability (run 1–3). To additionally evaluate the variability introduced by the PNGase F glycan release step, we processed a set of 16 independently released standards on the robotic system as well (day 4).

Analysis

Before the annotation of the obtained mass spectra, an internal calibration was performed by flexAnalysis 3.3 (Build 65, Bruker Daltonics) using a set of *N*-glycan calibration masses (**Table S1** in the Supporting Information). A full list of the detected glycan compositions is provided as **Table S2** in the Supporting Information. Figures were constructed using flexAnalysis, and annotation was performed according to CFG annotation using GlycoWorkbench[23].

For the analysis of the method repeatability, flexAnalysis was used to export all obtained mass spectra into the text format (x,y). The calibration of these exported files and the targeted extraction of the detected glycan compositions was performed by an in-house developed program “MassyTools”. Only spectra that showed a signal-to-noise ratio (S/N) of 9 or above (root-mean-square) for at least five calibration masses were included for further analysis. This method excluded all blanks (72) as well as 9 additional spectra. Furthermore, 20 spectra showing less than 70% of the analyte area above S/N values of 9 were excluded from analysis. For the remaining 779 spectra, the observed areas were normalized to the sum of all areas for each spectrum. For these normalized values, the averages were calculated per plate and day as well as the standard deviations (SDs) thereof. Derived traits were calculated using SPSS Statistics version 20 (IBM) (**Table S3** in the Supporting Information).

4.4 Results and discussion

Protocol implementation on an automated liquid handling platform

We here describe a new fully automated protocol that was implemented on a three-unit Hamilton robotic platform. The protocol is suitable for high-throughput studies on protein *N*-glycosylation by MALDI-TOF–MS involving sequential *N*-glycan release from plasma proteins with PNGase F, ethyl esterification, HILIC-SPE cleanup, and MALDI spotting[14]. The *N*-glycan release from plasma proteins with PNGase F is performed offline because this activity includes an overnight digestion step and does not necessarily benefit from an automation strategy. Further manual steps preceding automation include solution preparation and the placement of plates, pipetting tips, a tissue, and the aforementioned solutions on the robot deck. In addition, the scheduler software requires input on the amount of plates to process and tip numbers and locations, as well as the MALDI target spotting locations and volumes.

Compared to the manual version, the following adjustments were made: (1) chemical derivatization was carried out at room temperature; (2) instead of the previous Sepharose- or cotton-based approach, a GHP plate was used for the purification of esterified glycans; and (3) super-DHB was used as a MALDI matrix.

The sample handling on the robot starts with Unit2 loading the sample plates and processing plates onto Unit1 (step 1 in Figure 1), which in turn places the plates on the required deck positions. During transfer, the plate barcodes are read and saved in the database with the corresponding unique identifier. Through these barcodes, sample data can be imported from a sample list in either the laboratory information management system (LIMS), an Excel spreadsheet, or a text file. This sample list provides not only sample identification but also information on the number and location of samples in the plate to also allow the processing of partially filled plates.

After setup and loading, the first part of the ethyl esterification reaction (until the incubation step) is performed (step 2 in **Figure 1**). Using this setup, Unit1 is liberated for parallel actions during incubation. Following incubation, the addition of ACN and the subsequent purification by HILIC-SPE are performed as separate activities (step 3 in **Figure 1**), as well as the transfer of the resulting filter plate–PCR plate stack by Unit1 and Unit2 into the vacuum centrifuge (step 4 in **Figure 1**). After centrifugation, the stack is transferred to Unit3, the filter plate is discarded, and the eluted samples are spotted onto a MALDI target plate (step 5 in **Figure 1**). Finally, the sample and elution plates are stored in a plate stacker to make the positions available for the next experiment.

Elution of the glycans from the filter plate could alternatively be achieved by applying a vacuum to the GHP plate and collecting the flow-through. We experienced, however, that

droplets may stick to the nozzles of the filter plate, resulting in inconsistent elution volumes and sample loss. Therefore, we prefer a centrifugation procedure and indeed eliminated this problem. For similar reasons, the filter plate is pressed onto a piece of filter paper prior to building the PCR plate–filter plate stack to remove residual liquid from the bottom of the filter plate. A normal centrifuge is not incorporated in our system, but the centrifugal force of the vacuum centrifuge (approximately 300 *g* at a maximum speed of 1350 rpm for 5 min) proved sufficient to achieve complete elution and collection of the eluates in the PCR plate.

Eluates were mixed 1:1 with matrix solution on a separate 384-well plate and spotted on an AnchorChip MALDI target. We found that a high matrix ACN percentage was required to prevent the formation of air bubbles during mixing (leading to spotting inconsistencies). Eluates of a sample plate were directly spotted after the processing of that plate (1 h intervals) and left to dry by air. The resulting spots were analyzed by MALDI-TOF–MS in reflectron positive mode.

The processing of the sample plates on the robot was scheduled to include an overlap of procedures (see **Figure 2B**), allowing the parallel handling of multiple plates in a shorter time frame. This setup of the experiments is managed through an in-house developed Web site which stores the data in a mySQL database. The unique identifier is used here as a reference to the experiment (the sample plate). The current throughput allows the processing of 384 samples (four plates) using a total time of 7 h, including robot preparation and MALDI-TOF–MS measurement. Small changes in the deck layout of the STAR are expected to increase the uninterrupted sample throughput to 768 samples (eight plates) in 9.5 h.

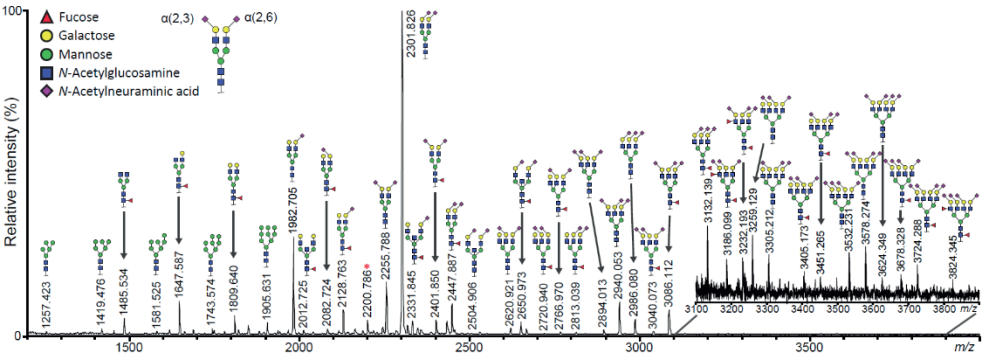

***Figure 3**. Reflectron positive-ion-mode MALDI-TOF–MS spectrum of released plasma N-glycome after robotic ethyl esterification, HILIC–SPE, and MALDI target spotting. Signals are assigned as [M + Na]⁺ glycan compositions on the basis of the observed mass and literature[24-27]. The N-acetylneuraminic acid linkage type could be determined by the mass spectrometric method, but monosaccharide positions and other displayed linkages are presumed on the basis of literature. The asterisk indicates an $^{0,2}A$ fragmentation of the main peak-reducing end N-acetylglucosamine.*

In summary, in this work, the implementation of a fully automated protocol was achieved on a three-unit Hamilton robotic system. Such application of multiple units provides time-efficient throughput; however, it is difficult to transfer to a different platform. Nevertheless, in principle, each part of the automated protocol can be implemented on hardware systems ("resources") from different manufacturers due to the modular design of the workflow (acknowledging that this requires specific adjustments and optimization strategies).

Repeatability testing

To prove the applicability and the advantages of the system, we performed experiments on three different days (day 1–3) with three 96-well sample plates per day (run 1–3). The sample plate used for the repeatability analysis contained 88 wells with a released plasma *N*-glycome standard from a single stock of mixed releases as well as 8 PBS blanks. In addition, separate releases were performed on 16 plasma samples to evaluate the added variation of the PNGase F release step (day 4). Obtained reflectron positive mode MALDI-TOF–MS spectra proved to be informative for the detection of 80 glycan compositions (average mass error 0.01 Da SD ± 0.01 Da), including various sialylated glycans separated by their linkage isomers (**Figure 3** and **Table S2** in the Supporting Information). In addition, no glycan signals were observed in any of the 72 blanks, indicating an absence of sample cross-contamination throughout the automated workflow.

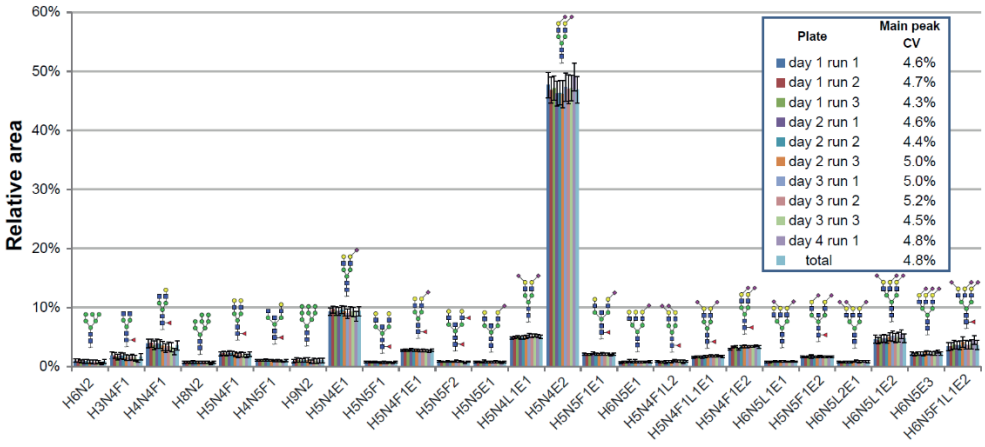

***Figure 4**. Repeatability of the robotized esterification workflow, represented by the relative profile of the 25 most abundant glycan compositions. A single mixture of released plasma N-glycome was distributed across a 96 well plate and subjected to the robotized sample preparation method for 3 days, 3 times per day, with subsequent MALDI-TOF–MS measurement. The fourth day was composed of 16 independent releases showing minimal contributions of the release step to the variation of the profiles. Error bars indicate standard deviation. H = hexose, N = N-acetylhexosamine, F = deoxyhexose (fucose), L = lactonized N-acetylneuraminic acid (α2,3-linked), E = ethyl esterified N-acetylneuraminic acid (α2,6-linked), CV = coefficient of variation.*

The consecutive analyses of the standard samples showed to be highly repeatable, both intraday (main peak averages per day being 47.2% (SD ± 2.2%), 46.2% (SD ± 2.2%), and 47.2% (SD ± 2.3%) of the total area of all assigned peaks) and interday (the main peak average across all days being 46.8% (SD ± 2.3%)) (**Figure 4** and **Figure S1** in the Supporting Information). The main peak coefficient of variation (CV) was, on average, 4.7% (SD ± 0.2%) but was generally higher for peaks that comprise a smaller portion of the total profile. For day 4, the main peak average was 49.0% (SD ± 2.4%, CV 4.8%), indicating a minor contribution of the PNGase F release to the profile repeatability. Method repeatability is at the level reported for manual preparation by a well-trained technician[14].

More clinically interesting than the individual relative glycan levels are the derived traits calculated from a subset of glycans. Examples of these include the percentage of high-mannose-type glycans (M), fucosylation of diantennary glycans (A2F), and sialylation of triantennary fucosylated glycans (A3FS) (Table S3 in the Supporting Information). Advantageously, these derived traits showed a higher repeatability than the individual traits from which they were calculated (Figure S2 in the Supporting Information). When we calculated 47 derived traits over the 779 spectra, the SDs were on average 1.6% (SD ± 0.8%). The average CV for the 43 derived traits with intensity values above 5% was 4.2% (SD ± 3.3%). The higher repeatability of the derived traits as compared to that of single glycan values might be due to the chemical similarity of the glycans contributing to the derived traits. This similarity may cause them to be similarly affected by small biases during the workflow (e.g., during HILIC-SPE, crystallization, or MS ionization), making ratios within them more robust than those obtained across a chemically more diverse spectrum of analytes (as is the case with individual glycan values relative to a total area or reference peak).

4.5 Conclusion

The objective of this study was to speed up and standardize glycan derivatization, purification, and analysis by MALDI-TOF–MS through automation using a robotic liquid-handling system. We were able to implement a time-efficient procedure on an automated system that showed to be highly repeatable with performance similar to or better than that of manual processing. Throughput times are 2.5 h for the first set of 96 samples and approximately 1 h extra for each additional sample plate. Automation of the protocol resulted in high intraday and interday repeatability, with standard deviations of the individual glycan compositions being below 3% on average and still lower for traits derived from those.

4.6 Supporting information

Figure S1: repeatability of the robotized esterification workflow for 80 detected glycan compositions. **Figure S2**: repeatability of derived glycosylation traits across all analyzed

spectra. **Table S1**: calibration masses. **Table S2**: compositions detected by reflectron positive mode MALDI-TOF–MS after robotized ethyl esterification. **Table S3**: derived glycan trait properties and calculations. The Supporting Information is available free of charge on the ACS Publications website at DOI: 10.1021/acs.jproteome.5b00538.

4.7 Acknowledgments

This work was supported by the Seventh Framework Programme projects HighGlycan (grant no. 278535) and IBD-BIOM (305479) of the European Union.

4.8 References

1 Crocker, P. R., Paulson, J. C. & Varki, A. Siglecs and their roles in the immune system. *Nat Rev Immunol* **7**, 255-266, doi:10.1038/nri2056 (2007).

2 Rudd, P. M., Elliott, T., Cresswell, P., Wilson, I. A. & Dwek, R. A. Glycosylation and the immune system. *Science* **291**, 2370-2376, doi:DOI 10.1126/science.291.5512.2370 (2001).

3 Varki, A. Biological roles of oligosaccharides: all of the theories are correct. *Glycobiology* **3**, 97-130 (1993).

4 Alessandri, L. *et al.* Increased serum clearance of oligomannose species present on a human IgG1 molecule. *MAbs* **4**, 509-520, doi:10.4161/mabs.20450 (2012).

5 Jefferis, R. Glycosylation as a strategy to improve antibody-based therapeutics. *Nature Reviews Drug Discovery* **8**, 226-234, doi:10.1038/nrd2804 (2009).

6 Adamczyk, B., Tharmalingam, T. & Rudd, P. M. Glycans as cancer biomarkers. *Bba-Gen Subjects* **1820**, 1347-1353, doi:10.1016/j.bbagen.2011.12.001 (2012).

7 Albrecht, S., Unwin, L., Muniyappa, M. & Rudd, P. M. Glycosylation as a marker for inflammatory arthritis. *Cancer Biomark* **14**, 17-28, doi:10.3233/CBM-130373 (2014).

8 Guillard, M. *et al.* Plasma N-glycan profiling by mass spectrometry for congenital disorders of glycosylation type II. *Clin Chem* **57**, 593-602, doi:10.1373/clinchem.2010.153635 (2011).

9 Shubhakar, A. *et al.* High-Throughput Analysis and Automation for Glycomics Studies. *Chromatographia* **78**, 321-333, doi:10.1007/s10337-014-2803-9 (2015).

10 Doherty, M. *et al.* An automated robotic platform for rapid profiling oligosaccharide analysis of monoclonal antibodies directly from cell culture. *Anal Biochem* **442**, 10-18, doi:10.1016/j.ab.2013.07.005 (2013).

11 Stockmann, H., Adamczyk, B., Hayes, J. & Rudd, P. M. Automated, High-Throughput IgG-Antibody Glycoprofiling Platform. *Anal Chem* **85**, 8841-8849, doi:10.1021/ac402068r (2013).

12 Harvey, D. J. Matrix-assisted laser desorption/ionization mass spectrometry of carbohydrates. *Mass Spectrom Rev* **18**, 349-450, doi:10.1002/(SICI)1098-2787(1999)18:6<349::AID-MAS1>3.0.CO;2-H (1999).

13 Huffman, J. E. *et al.* Comparative performance of four methods for high-throughput glycosylation analysis of immunoglobulin G in genetic and epidemiological research. *Mol Cell Proteomics* **13**, 1598-1610, doi:10.1074/mcp.M113.037465 (2014).

14 Reiding, K. R., Blank, D., Kuijper, D. M., Deelder, A. M. & Wuhrer, M. High-throughput profiling of protein N-glycosylation by MALDI-TOF-MS employing linkage-specific sialic acid esterification. *Anal Chem* **86**, 5784-5793, doi:10.1021/ac500335t (2014).

15 Anthony, R. M. *et al.* Recapitulation of IVIG anti-inflammatory activity with a recombinant IgG Fc. *Science* **320**, 373-376, doi:10.1126/science.1154315 (2008).

16 Kannagi, R. Molecular mechanism for cancer-associated induction of sialyl Lewis X and sialyl Lewis A expression - The Warburg effect revisited. *Glycoconj J* **20**, 353-364, doi:Doi 10.1023/B:Glyc.0000033631.35357.41 (2003).

17 Takada, A. *et al.* Contribution of Carbohydrate Antigens Sialyl Lewis-a and Sialyl Lewis-X to Adhesion of Human Cancer-Cells to Vascular Endothelium. *Cancer Res* **53**, 354-361 (1993).

18 Bondt, A. *et al.* Immunoglobulin G (IgG) Fab glycosylation analysis using a new mass spectrometric high-throughput profiling method reveals pregnancy-associated changes. *Mol Cell Proteomics* **13**, 3029-3039, doi:10.1074/mcp.M114.039537 (2014).

19 Burnina, I., Hoyt, E., Lynaugh, H., Li, H. J. & Gong, B. A cost-effective plate-based sample preparation for antibody N-glycan analysis. *J Chromatogr A* **1307**, 201-206, doi:10.1016/j.chroma.2013.07.104 (2013).

20 Ruhaak, L. R. *et al.* Hydrophilic interaction chromatography-based high-throughput sample preparation method for N-glycan analysis from total human plasma glycoproteins. *Anal Chem* **80**, 6119-6126, doi:10.1021/ac800630x (2008).

21 Bladergroen, M. R. *et al.* Standardized and automated solid-phase extraction procedures for high-throughput proteomics of body fluids. *J Proteomics* **77**, 144-153, doi:10.1016/j.jprot.2012.07.023 (2012).

22 van den Broek, I. *et al.* Quantification of serum apolipoproteins A-I and B-100 in clinical samples using an automated SISCAPA-MALDI-TOF-MS workflow. *Methods* **81**, 74-85, doi:10.1016/j.ymeth.2015.03.001 (2015).

23 Ceroni, A. *et al.* GlycoWorkbench: a tool for the computer-assisted annotation of mass spectra of glycans. *J Proteome Res* **7**, 1650-1659, doi:10.1021/pr7008252 (2008).

24 Kornfeld, R. & Kornfeld, S. Assembly of Asparagine-Linked Oligosaccharides. *Annu Rev Biochem* **54**, 631-664, doi:DOI 10.1146/annurev.biochem.54.1.631 (1985).

25 Nairn, A. V. *et al.* Regulation of glycan structures in animal tissues: transcript profiling of glycan-related genes. *J Biol Chem* **283**, 17298-17313, doi:10.1074/jbc.M801964200 (2008).

26 Saldova, R. *et al.* Association of N-glycosylation with breast carcinoma and systemic features using high-resolution quantitative UPLC. *J Proteome Res* **13**, 2314-2327, doi:10.1021/pr401092y (2014).

27 Stumpo, K. A. & Reinhold, V. N. The N-glycome of human plasma. *J Proteome Res* **9**, 4823-4830, doi:10.1021/pr100528k (2010).